

**This item is the archived peer-reviewed author-version of:**

Dual microfluidic sensor system for enriched electrochemical profiling and identification of illicit drugs on-site

**Reference:**

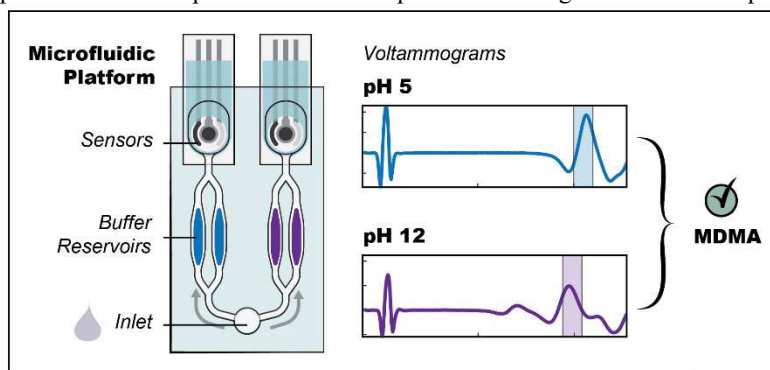
Steijlen Annemarijn, Parrilla Pons Marc, Van Echelpoel Robin, De Wael Karolien.- Dual microfluidic sensor system for enriched electrochemical profiling and identification of illicit drugs on-site  
Analytical chemistry - ISSN 1520-6882 - 96:1(2024), p. 590-598  
Full text (Publisher's DOI): <https://doi.org/10.1021/ACS.ANALCHEM.3C05039>  
To cite this reference: <https://hdl.handle.net/10067/2018770151162165141>

# Dual Microfluidic Sensor System for Enriched Electrochemical Profiling and Identification of Illicit Drugs On-Site

Annemarijn S. M. Steijlen, Marc Parrilla, Robin Van Echelpoel, Karolien De Wael\*

A-Sense Lab, Department of Bioscience Engineering, University of Antwerp, Groenenborgerlaan 171, 2020 Antwerp, Belgium

**ABSTRACT:** Electrochemical sensors have emerged as a new analytical tool for illicit drug detection to facilitate ultra-fast and accurate identification of suspicious compounds on-site. Drugs of abuse can be identified using their unique voltammetric fingerprint at a given pH. Today, the right buffer solution is manually selected based on drug appearance and in some cases a consecutive analysis in two different pH solutions is required. In this work, we present a disposable microfluidic multi-channel sensor system that automatically records fingerprints in two pH solutions (e.g. pH 5 and pH 12). This system has two advantages. It will overcome the manual selection of a buffer solution at the right pH, decrease analysis time and minimize the risk of human errors. Second, the combination of two fingerprints, the superfingerprint, contains more detailed information about the samples, which enhances the selectivity of the analytical technique. First, real-time pH measurements proved that the sample can be brought to the desired pH within a minute. Subsequently, an electrochemical study on the microfluidic platform with 1 mM illicit drug standards of MDMA, cocaine, heroin and methamphetamine showed that the characteristic voltammetric fingerprints and peak potentials are reproducible, also in the presence of common cutting agents. Finally, the microfluidic concept was validated with real confiscated samples showing promising results for the user-friendly identification of drugs of abuse. In short, this paper presents a successful proof-of-concept study of a multi-channel microfluidic sensor system to enrich the fingerprints of illicit drugs at pH 5 and pH 12, thus providing a low-cost, portable, and rapid identification system of illicit drugs with minimal user intervention.



The use of psychoactive drugs is associated with serious health risks.<sup>1</sup> The United Nations Office of Drugs and Crime estimated that in 2020, 284 million people between 15 and 64 years old used drugs in the previous 12 months. Cannabis is the most frequently used drug with an estimated 209 million users in 2019. Opioids like heroin account for the most significant harm. Opioids were used for non-medical reasons by approximately 61 million people in 2019, followed by amphetamine-type stimulants (34 million) and cocaine (21 million users).<sup>2</sup> In 2020, over 350 production facilities were found in Europe and numbers of drug seizures are hitting records.<sup>3</sup> Therefore, the reduction of illicit drug production, trafficking and use are key challenges for the European governments.

In order to intercept illicit drugs and identify drug trafficking routes, there is a need for fast and reliable on-site detection systems. Current handheld systems, often used by border officers, include color tests<sup>4</sup> and portable spectroscopic systems.<sup>5</sup> However, in the case of colored samples or the presence of certain cutting agents, these systems often produce unreliable results.<sup>6</sup>

Although novel spectroscopic alternatives based on near-infrared technology are developed to overcome color interference,<sup>7,8</sup> alternative on-site electrochemical detection methods are emerging. The detection method is based on the characteristic electrochemical profile of each compound, recorded using square wave voltammetry.<sup>9</sup> Provided that the right pH strategy is used, key illicit drugs such as cocaine, heroin, methamphetamine, 3,4-methylenedioxymethamphetamine -MDMA-, and ketamine can be detected. Heroin and MDMA can be detected at pH 5 and pH 12<sup>10,11</sup> and cocaine and methamphetamine at pH 12 but not at pH 5.<sup>12,13</sup> Currently the technique relies on manual selection of the buffer solution with the right pH by the operator based on a first visual inspection of the suspicious sample.<sup>14</sup>

In this paper, we introduce for the first time the design of a disposable microfluidic platform that will automatically bring the sample solution to the right pH and transports it to the electrochemical sensor (i.e. screen-printed electrodes). Hence, the multi-channel platform can be used to simultaneously perform an electrochemical measurement at different pH levels. The

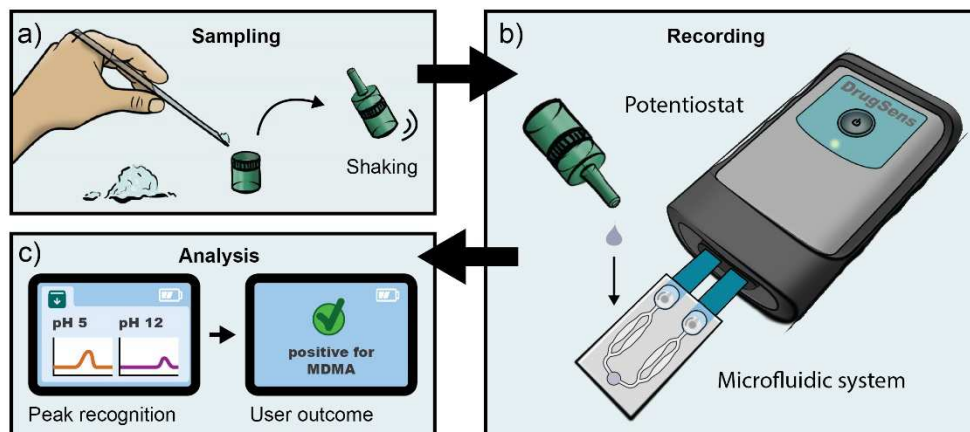


**Figure 1.** Concept illustration. A) The user adds a small amount of the sample to the ampoule with 0.1 M KCl in water and shakes it. B) A droplet is placed at the inlet of the microfluidic system. The microfluidic system brings the sample to the right pH and transports it to the sensor chambers. A dual measurement is performed with one potentiostat. C) Measurements at two different pH values result in a superfingerprint of the sample. The algorithm analyses the superfingerprint and tells the user whether an illicit drug is found.

results will be combined to create a superfingerprint of the two signals to identify the different illicit drugs automatically.

The concept of the illicit drug detection platform is presented in **Figure 1**. In the case a suspicious compound is found, a small amount is collected with a spatula and placed in an ampoule to dissolve it in demineralized water with 0.1 M KCl (**Figure 1a**). The user is requested to shake the ampoule and to add one droplet (ca 90  $\mu$ L) at the inlet of the microfluidic system, which is then placed in the handheld MultiPalmSens4 potentiostat (PalmSens, the Netherlands) (**Figure 1b**). Once the system is completely filled, i.e. the two electrodes are completely covered, a dual square wave voltammetric measurement is performed. Two fingerprints of the substance are recorded (**Figure 1c**) at pH 5 and at pH 12 respectively. Together they form the superfingerprint. A tailored algorithm applies a baseline correction and a top hat filter<sup>15</sup> to the recordings for an easier identification of the peak potentials. Subsequently, it checks whether the set of peak voltages corresponds to the illicit reference measurements from the database, and thereafter, a clear indication of the presence or absence of the illicit drugs is given.

To reduce the time of analysis and improve the automation of the electrochemical procedure, different concepts of microfluidic designs can be deployed for a new automated buffer supply system. Microfluidic design concepts can be organized by fabrication method. Common fabrication methods to create microfluidic channels include casting polydimethylsiloxane (PDMS)<sup>16,17</sup> or laminating polymer foils.<sup>18</sup> Furthermore, various paper-based microfluidic structures, also known as  $\mu$ pads<sup>19,20</sup>, have been developed in recent years. Regarding paper-based systems as well as PDMS or foil-based systems, different strategies can be identified for automatic reagent addition and optimal mixing. For PDMS and laminated foil structures, a large range of concepts can be found where liquid reagents are supplied via different inlets, after which passive mixing is realized by smart geometry changes in the channel.<sup>21</sup> For example, by creating a sinusoidal microchannel,<sup>22</sup> Tesla valves,<sup>23</sup> staggered bars<sup>24</sup> or even 3D structures.<sup>25</sup> Paper-based structures gained interest for their ability to store reagents for multistep processes. The lateral flow assay<sup>26,27</sup> is a widely used system for point-of-care solutions and even enables the integration of nanomaterials for receptor immobilization.<sup>28</sup> Fu et al. developed a paper-

based system for malaria antigen detection that sequentially adds the sample and conjugated antibody, a rinse buffer and a signal amplification reagent.<sup>29</sup> A disadvantage for commercial use of this system by laymen is that three well-defined amounts of liquid need to be added to three different inlets by the user.

Our new microfluidic system with electrochemical sensors for illicit drug detection requires the integration of three consecutive steps: i) the addition of the dissolved sample ii) bringing the dissolved sample to the desired pH and iii) the voltammetric analysis. Laminated foils are easy to fabricate and facilitate quick iterations of the microfluidic design. Furthermore, we aim to avoid the risk of entrapment of air at the sensor surface and to minimize the risk of contact of a paper medium with the sensor surface. Therefore, a hydrophilic foil-based system is designed. First, the design of the patch including a flow simulation is presented. Second, a pH 5 single channel microfluidic system is built and real-time pH measurements are performed in the sensor chamber to analytically assess whether the desired pH value of 5 can be guaranteed. Third, the concept is expanded to a dual buffer system (pH 5 and pH 12) and tested with standard solutions of four of the most common illicit drugs, i.e. MDMA, cocaine, heroin and methamphetamine. Voltammograms of the four drugs with cutting agents are recorded to simulate street compositions. Finally, a validation with 20 confiscated samples previously analyzed by forensic standard methods is performed to evaluate the reliability of the microfluidic system.

## Experimental section

### Reagents and Materials

Analytical grade reagents of citric acid, sodium citrate dihydrate, potassium chloride, potassium phosphate and sodium hydroxide were purchased from Sigma-Aldrich (Merck, Belgium). For pH 5, a citrate buffer with citric acid and sodium citrate dihydrate was made. For pH 12, a phosphate buffer with disodium hydrogen phosphate, potassium dihydrogen phosphate and sodium hydroxide was made. 18.2 M $\Omega$ /cm doubly deionized water (Milli-Q, Merck Millipore) was used to make the solutions. Standards of four of the most common illicit drugs: 3,4-methylenedioxymethamphetamine HCl (MDMA), cocaine HCl, heroin HCl and methamphetamine HCl were acquired from Chiron AS, Norway. The cutting agents

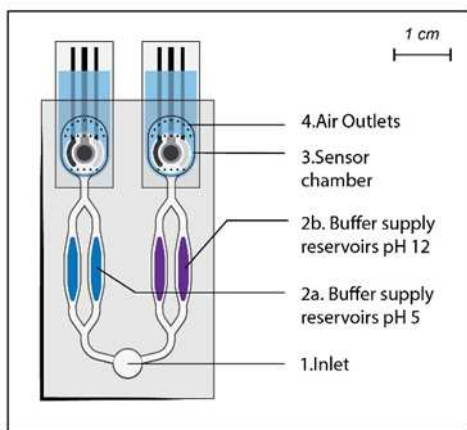


**Figure 2.** Detailed design of the microfluidic system integrated on the screen-printed electrodes for simultaneous dual pH analysis.

paracetamol, caffeine, lidocaine, levamisole and phenacetine, as well as the confiscated samples were supplied by NICC, the National Institute for Criminalistics and Criminology in Belgium. The confiscated sample composition was analyzed by NICC with a standardized gas chromatography-mass spectrometry procedure. The microfluidic channels were created with a highly hydrophilic foil (ARflow® 93361) and a double-side adhesive (ARcare® 8939) both from Adhesives Research Inc., Ireland. Both materials are polyester films with a top hydrophilic layer and adhesive layers respectively. Disposable Italsens IS-C Screen Printed Electrodes (SPEs) (PalmSens, the Netherlands) were integrated into the microfluidic channels. The potentiometric pH measurements were performed with custom-made screen printed electrodes with carbon working electrodes (Sunchemical, United States) modified with aniline and HCl (Sigma-Aldrich, Belgium). Reagents for the flow experiments and pH measurements include brilliant black and thymol blue sodium salt (Sigma-Aldrich, Belgium).

### Instrumentation and apparatus

Voltammetry and potentiometry were performed with a Multi-PalmSens4 and EmStat4R potentiostat (PalmSens, the Netherlands). Square wave voltammetry between -0.1 and 1.5 V (5 mV step potential, 25 mV amplitude and a frequency of 10 Hz) was used. All voltammetric measurements in this manuscript are performed in 0.1 M KCl solution with the screen-printed electrodes, containing a graphite working electrode (3 mm diameter), a carbon counter electrode and a silver (pseudo) reference electrode. Voltammograms were background corrected using the moving average baseline correction tool in PSTRace software (PalmSens, The Netherlands). To analyze the confiscated sample voltammograms, peak separation was enhanced using a top-hat filter written in Matlab (MathWorks, United States). Reference measurements were performed in a 90  $\mu$ L droplet of 20 mM 0.1M KCl buffer solutions. The foils of the new microfluidic systems were cut in the desired shape with a general-purpose vinyl cutter (Silhouette Cameo 4, United States) and assembled manually.

### Microfluidics design

**Figure 2** shows the detailed design of the microfluidic system. A droplet of the dissolved analyte is placed on the inlet of the microfluidic system (**Figure 2**, nr.1). Capillary forces ensure the inflow of the sample fluid in the first reservoirs (**Figure 2**, nr. 2,

thickness = 126  $\mu$ m). These reservoirs contain buffer salts that adjust the sample to the desired pH. Afterward, the sample enters the sensor chambers (**Figure 2**, nr. 3, thickness = 380  $\mu$ m) where a square wave voltammogram is recorded. The supply channel branches into two channels to increase the capillary pressure<sup>30</sup>, ensuring the complete filling of the sensor chamber. In the two buffer reservoirs on the left side, a buffer solution pH 5 based on sodium citrate dihydrate and citric acid is added to each reservoir. On the right side, a buffer solution with pH 12 based on potassium phosphate is added to both reservoirs. The reagents are deposited in the system by drop casting 2.6  $\mu$ L of concentrated buffer solution (100 mM) in each buffer supply reservoir and left to dry at room temperature. Given that the sensing reservoir is 26  $\mu$ L, the desired buffer capacity of 20 mM will be reached when the sample is added. The detailed assembly process is depicted in Supporting Information **Figure S1**.

### Simulation and flow tests

Capillary forces ensure the inflow of the sample in the microfluidic system. The capillary pressure is dependent on the dimensions of the microchannel and the surface tension, as explained by the Young-Laplace equation. To decrease the contact angle of the walls, highly hydrophilic foils were chosen. However, the sensor surface is more hydrophobic, which may result in a flow along the edges and entrapment of air above the sensor. To analyze this effect and optimize the air outlets of the design, computational fluid dynamics (CFD) simulations of the measurement chamber were performed in COMSOL Multiphysics software with two different designs. The level set function for movement of the fluid interface and the Navier Stokes equations for mass and momentum transport are used in this simulation.<sup>31</sup> Initially, the sensor chamber is filled with air and water can move freely into the channel. Hydrostatic pressure is added and the wetted wall feature is used to define the hydrophilic and hydrophobic areas. A longitudinal symmetry plane is defined in the sensor reservoir to minimize computational time. To test the final concept, two flow experiments were performed. First, the inflow of the sample was tested by drop-casting demineralized water dyed with 1mg/ml brilliant black. Second, pH indicator experiments with a 2 mM thymol blue sodium salt solution with 3 mM HCl were performed.

### Fabrication of a potentiometric pH sensor

Once the design was established, miniaturized pH electrodes were fabricated to measure the pH in the sensor chamber. To create pH sensitive sensors, electrodeposition of polyaniline (PANI)<sup>32,33</sup> on our custom screen-printed carbon electrodes was chosen. Cyclic voltammetry between -0.2 and 1.2 V was performed at a scan rate of 0.025 V/s in 0.1M aniline 1 M HCl to electrodeposit a PANI layer. The number of cycles was optimized based on the response time of the sensors. The sensors were dried overnight and they were conditioned for three hours before use. After calibration with Britton Robinson buffers from pH 4 to pH 8, they were placed in the microfluidic system. Measurements with 0.1 M KCl solution in the microfluidic system were performed to test the use of reservoirs to achieve different pHs in the sensor chambers.

### Electrochemical analysis of illicit drugs

The analytical evaluation consists of three parts. First, the superfingerprints of 1 mM standards of four illicit drugs: MDMA, cocaine, heroin, and methamphetamine, in 0.1 M KCl, are recorded with the new microfluidic system. Three new microfluidic systems are used for each measurement to test the reproducibility. Based on these measurements, characteristic peak

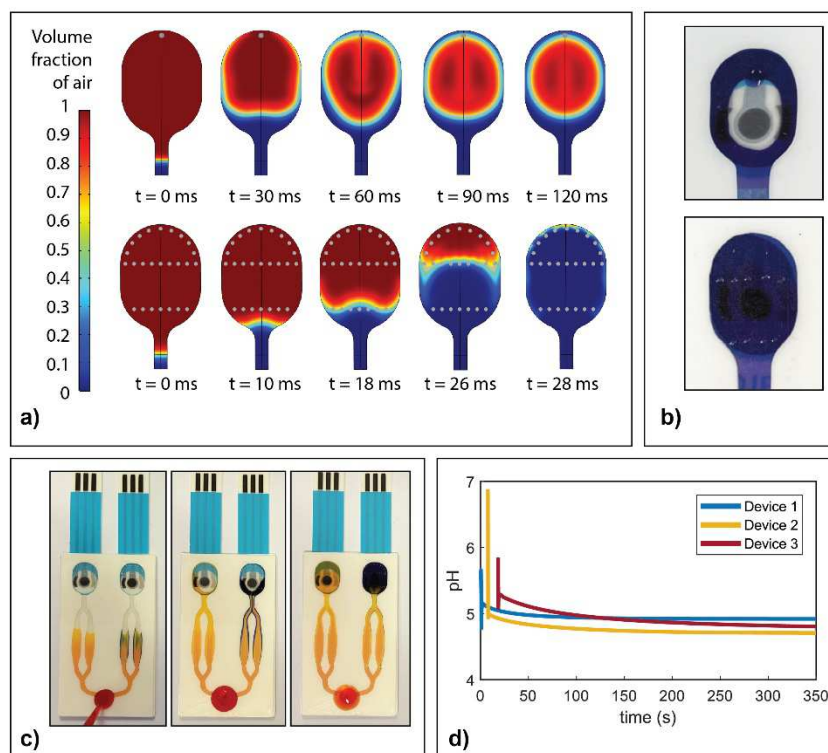


**Figure 3.** a) Simulations of the volume fraction of air in the sensor chamber at different time points during the filling process. The top row shows the results of a system with one air outlet (grey dots). The bottom row shows the results of a system with multiple air outlets (grey dots). b) Result of the filling process with a brilliant black solution for the single air outlet system (top) and the multiple air outlet system (bottom). c) Pictures of the filling process with thymol blue solution (at 5 s, 10 s and 30 s). The colors indicate that in the left reservoirs the pH is shifted to a pH above 2.5 and in the right reservoirs to a pH above 9. d) Real-time pH measurement during the filling process with a custom-made PANI sensor located in the left sensor chamber. The pH value stabilizes at pH 5 within 50 seconds for all three devices.

potential detection windows for each illicit drug are determined. For each drug, two reference measurements of 1 mM standard in 20 mM citrate buffer pH 5 and 20 mM PBS buffer pH 12 are performed to compare with the results from the microfluidic system. In a second series of experiments, binary mixtures (equimolar, 1 mM) of the illicit drug standards and the most common cutting agents are recorded in new microfluidic systems to test whether the characteristic peaks of the illicit drugs can still be identified in the solutions with cutting agents. Third, the superfingerprints of five confiscated samples of each of the four drugs are recorded with new microfluidic systems, to find out whether the drugs can be identified in real samples. The confiscated samples are prepared by making solutions of 1 mg/ml in demineralized water with 0.1 M KCl. For methamphetamine samples, higher concentrations of 5 mg/ml were used, except for the liquid sample (nr. 20).

## Results & Discussion

### Assessment of the filling process

Because the sensor surface is hydrophobic compared to the materials of the microfluidic system, the sensor reservoir tends to fill along the edges. This leads to the entrapment of air in the sensor chamber **Figure 3a** shows a simulation of how the air will be entrapped when there is only one air outlet at the top of the reservoir. Therefore, it was decided to create an alternative design for the air outlets. This design consists of a row of air outlets below and above the sensor surface (**Figure 2**). As shown in the second simulation, this design forces the fluid-air interface to move in a more horizontal direction from bottom to top. This results in a completely filled system, avoiding

entrapment of air at the electrode surface (**Figure 3a**). **Figure 3b** shows the results of a fluid flow experiment. Inflow was monitored when a 50  $\mu$ l brilliant black solution is pipetted at the inlet. These experiments prove that the simulations correspond to reality and the system with multiple air outlets fills in the desired way. A second flow experiment was performed with the pH indicator thymol blue. **Figure 3c** shows three pictures of the inflow of the thymol blue solutions at three points in time. The pictures show that the buffer addition reagents dissolve directly and the color change indicates that the pH on the left side shifts to a pH above 2.5 but below pH 9 and at the right side to a pH above 9, since these are the indicator endpoints (i.e.  $pK_{in}$ ) of thymol blue.<sup>34</sup> There is a slight gradient visible in the sensor chamber, when you zoom in at the picture at the right. However, due to their lower molecular weight, the diffusion rate for the buffer salts will be higher (as explained by Graham's law), which will result in faster homogeneous distribution of the buffer compounds.

### Real-time pH measurement

During the fabrication process of the pH sensors, the number of voltammetric cycles was varied between 24, 12 and 6 cycles. It was concluded that electrodes with PANI deposited for just 6 cycles resulted in the fastest response time and excellent repeatability (**Figure S2**). Once the optimal electrodeposition was selected, the analytical characterization of the pH sensors was executed. **Figure S3a** shows the time trace of the pH sensor upon pH changes in the solution exhibiting excellent reversibility with a short time of response. Importantly, potentiometric measurements showed a linear relationship from pH 4 to pH 8 (**Figure S3b**). This confirms that the sensors can be applied to

test whether the pH 5 buffer addition system works. After characterization, the sensor was placed in the microfluidic system. A 0.1 M KCl solution was added to the system and the pH was recorded for 350 seconds. Three systems were fabricated to test the reproducibility. **Figure 3d** shows that the pH of all three systems goes to pH 5 within approximately 50 seconds. Although the pH slightly varied between replicates from pH 4.72 to pH 4.92, the experiment proves the ability of the microfluidic system to attain ca. pH 5 values which is sufficient for the purpose of analyzing a voltammogram for drug analysis at pH 5.<sup>35</sup>

#### Analytical characterization of the microfluidic device

From previous work, it is known that the four selected illicit drugs are electroactive.<sup>14</sup> In most cases, this electroactive behavior can be explained by the oxidation of secondary and tertiary amines on a carbon-based electrode, resulting in a peak at a potential between 0 and 1.2 V. Triplicate measurements of 1 mM drug standards (MDMA, cocaine, heroin and methamphetamine) in 0.1 M KCl solution were performed using every time a new microfluidic system (**Figure 4**). The recordings were compared with a reference measurement of 1 mM standard in buffer solution pH 5 and pH 12 on a bare electrode (using a droplet of 90  $\mu$ L) (dotted lines in **Figure 4**).

The results for MDMA (**Figure 4a**) showed that the MDMA peak is clearly visible ( $E_p=1.054 \pm 0.004$  V,  $N=3$ ) and even shows a higher peak current with respect to the reference. As shown in **Figure S4**, this can be explained by the presence of a surfactant on the hydrophilic foil, which can improve the electrochemical oxidation of the drugs at the electrode.<sup>36,37</sup> Although the peak intensity varies due to the presence of surfactants, the peak potential is reproducible between measurements (max. difference = 10 mV, see **Table S1**). At pH 12, the MDMA peak contains a shoulder in the reference measurement, which becomes a separated peak in the microfluidic systems. Previous work explained that this first peak is attributed to the secondary amine oxidation process, while the second peak ( $E_p=0.991 \pm 0.008$  V,  $N=3$ ) shows the oxidation of the methylenedioxy group.<sup>14</sup> For cocaine (**Figure 4b**), there is no peak linked to the presence of cocaine at pH 5, while at pH 12 there is a clear peak at 0.802 V, which is similar to results in literature.<sup>38</sup> The cocaine peak is slightly asymmetrical and shifted towards a more negative potential compared to the reference (a 0.06 V shift) which is most probably caused by the surfactant present on the hydrophilic foil. The difference in intensity might be explained by an uneven distribution of surfactant across the foil, resulting in different concentrations of the analyte in each sample. For the heroin standards (**Figure 4c**), a characteristic peak is identified at both pHs (pH 5 mean  $E_p=0.996 \pm 0.005$  V,  $N=3$ , pH 12 mean  $E_p=0.761 \pm 0.010$  V,  $N=3$ ). At pH 12, the fingerprints of the heroin standard usually show two characteristic peaks. In alkaline conditions, heroin degrades resulting in the formation of 6-monoacetylmorphine (6-MAM). This explains the first peak (i.e.  $E_p=0.160$  V) in the reference measurement at pH 12.<sup>39</sup> In the microfluidic system, the measurement is performed directly after bringing the sample to pH 12. There is less time for degradation, explaining the very small 6-MAM peak (**Figure 4c, pH 12**). To confirm this hypothesis, the measurement was performed in a new microfluidic system 20 min after the sensor reservoir was filled. **Figure S5** shows that the 6-MAM peak is indeed clearly visible when the measurement is performed later. As can be seen in **Table S1**, the heroin peaks are close to the mean peak values of cocaine and MDMA. This confirms the need for measuring the drugs at two pH values, which results in a more unique fingerprint for each analyte.

Previous research of the fingerprints of methamphetamine showed a significant shift of the peak potential to lower voltages at higher concentrations.<sup>13</sup> Furthermore, it was demonstrated that a higher sample amount (7.5 mM) resulted in more reliable detection of methamphetamine in the presence of other compounds. Therefore, both 1 mM and 7.5 mM methamphetamine

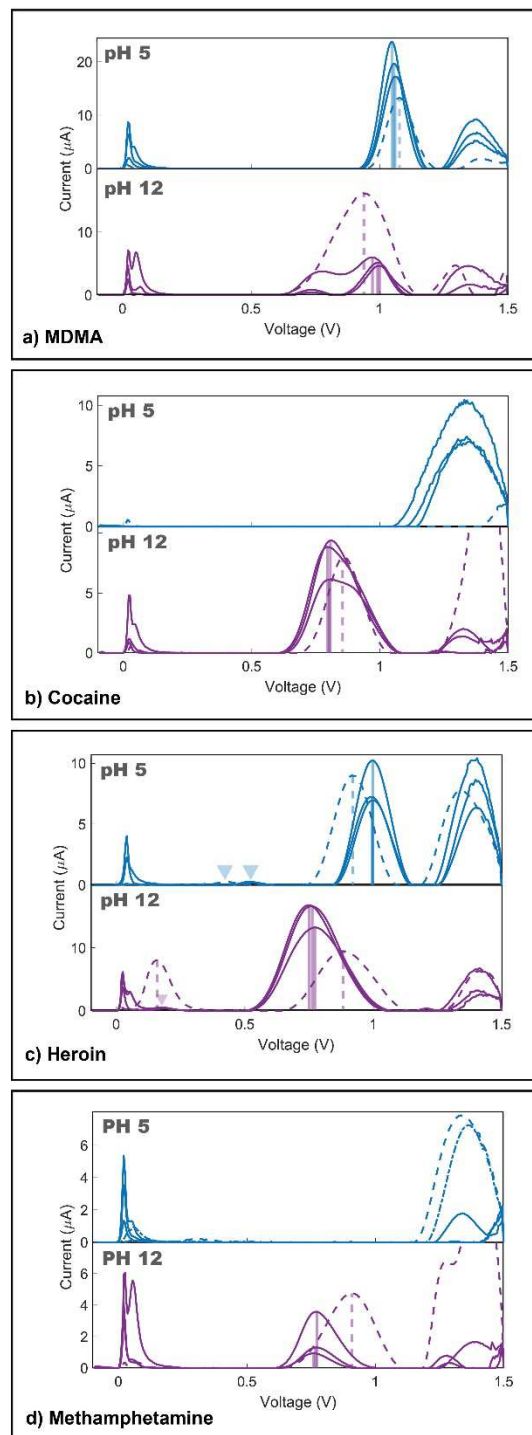


**Figure 4.** Triplicate measurements (at pH 5 and pH 12) of 1 mM of a) MDMA, b) cocaine, c) heroin and d) methamphetamine in the new microfluidic system. Dotted lines are reference measurements of 1mM illicit drug in buffer pH 5 and buffer pH 12 solutions obtained at a bare electrode without microfluidics. Vertical lines indicate the characteristic peak potentials of each drug.

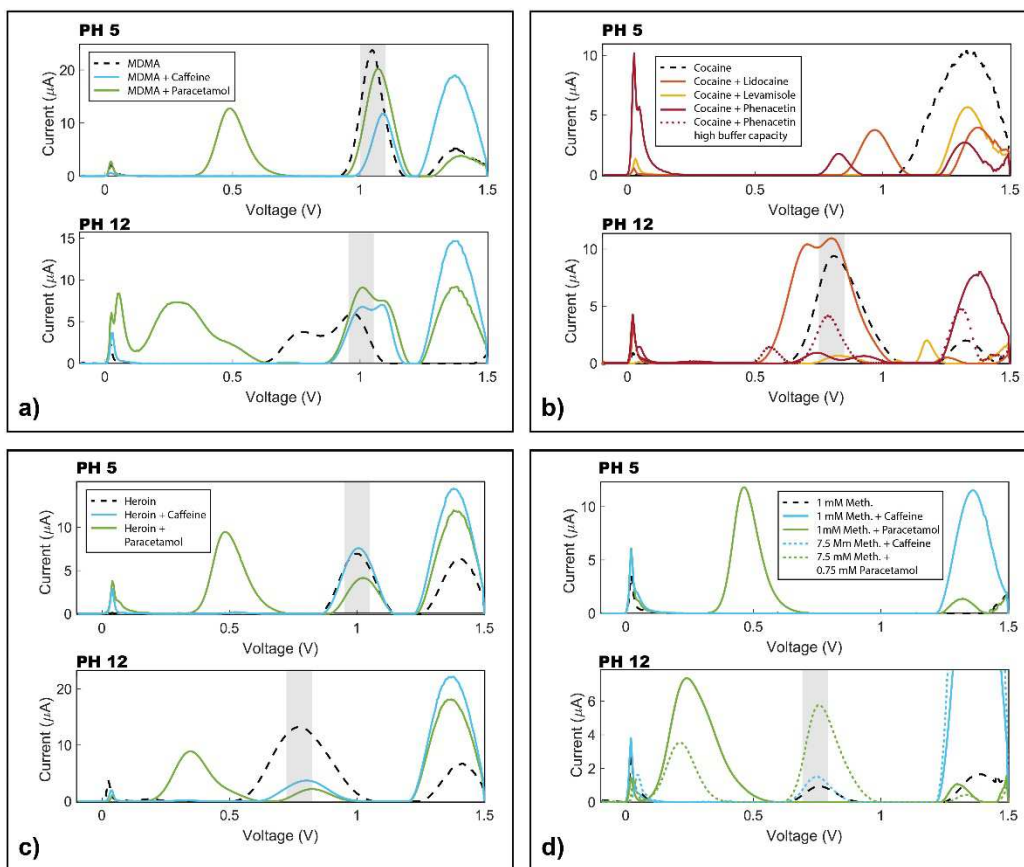


**Figure 5.** Electrochemical fingerprints of equimolar (1 mM) binary mixtures of a) MDMA, b) cocaine, c) heroin and d) methamphetamine and common cutting agents after moving average baseline correction. Measurements were performed in the microfluidic system, bringing the sample pH 5 and pH 12. The dotted lines show the fingerprints of 1 mM drug standard in the microfluidic system. The grey bars indicate the potential window for identifying the drugs.

standard solutions were tested in the microfluidic system. In **Figure 4d**, the 1 mM measurements are shown. A characteristic peak can be identified at pH 12 (mean  $E_p = 0.767 \pm 0.002$  V,  $N=3$ ), and no peaks are detected at pH 5, corresponding to literature.<sup>13</sup> **Figure S6** shows the 7.5 mM results as well. For the higher concentration, the mean peak value shifted not significantly ( $0.027 \pm 0.006$  V,  $N=3$ ) in the microfluidic system. In short, reproducible characteristic fingerprints of all four illicit drugs were successfully obtained using the microfluidic electrochemical system.

**Figure 5** depicts the electrochemical profiles of the binary mixtures of drugs with cutting agents. As shown in **Figure 5a**, MDMA peaks can still be recognized in the presence of caffeine and paracetamol. For the binary mixtures with cocaine (**Figure 5b**), the peaks are suppressed in the presence of levamisole and phenacetin. This corresponds to the effects reported in literature.<sup>12</sup> Phenacetin oxidizes at a lower potential than cocaine and will release protons. In the presence of these protons cocaine cannot oxidize, which results in suppression of the cocaine peak.<sup>38</sup> The microfluidic reservoir enlarges this effect, since the thin reservoir inhibits diffusion of these protons away from the electrode surface. To test whether an increased buffer capacity could diminish this effect, a test was performed in a microfluidic system with a higher buffer capacity (80 mM instead of 20 mM). The dotted red line in **Figure 5b** shows that a clear cocaine peak appears when the buffer capacity is increased. This indicates that the performance of the sensor system will increase for cocaine when there is a stronger buffer capacity. For heroin

(**Figure 5c**), the paracetamol peak overlaps with the 6-MAM peak, which was already reported in literature.<sup>39</sup> Fortunately, the heroin peak is visible in the presence of both cutting agents. Methamphetamine binary mixtures were made at 1 mM and 7.5 mM. For the equimolar 1 mM binary mixtures, the methamphetamine peak was not identified (**Figure 5d**). In contrast, at 7.5 mM, the characteristic methamphetamine peak can be detected in the presence of caffeine. Similarly, the peak is not visible in an equimolar mixture with paracetamol. Nevertheless, in literature it is reported that the relative amount of paracetamol in seized samples is 10% at maximum.<sup>13,40</sup> When the mixture contains 0.75 mM of paracetamol, the methamphetamine peak is clearly visible as shown by the green dotted line in **Figure 5d**.

To validate the functioning of the microfluidic system, five confiscated samples of each illicit drug were analyzed. Information about the composition of the confiscated samples from the standard GC-MS analysis performed at NICC can be found in **Table S2**. The voltammograms of these samples were processed with a top-hat filter, which enhances the separation of overlapping peaks originating from cutting agents and precursors.<sup>41</sup> **Figure 6** shows the superfingerprints of MDMA, cocaine, heroin and methamphetamine. The MDMA samples (**Figure 6a**) all exhibit the characteristic MDMA peak at both pH 5 and pH 12. However, for pH 5 the peak is slightly shifted to a higher potential. This can be explained by the high purity of samples 2-4 (Table S2). Higher sampling of MDMA can lead to a shift to higher potentials.<sup>11</sup> To successfully detect these

samples as well, the potential window may be widened. The increase of false positives by widening the potential window will be minimal compared to the single pH system, because the measurements at two different pHs will be combined to draw a conclusion. In **Figure 6b** it is shown that only three out of five cocaine peaks could be identified. For sample 7, cocaine was probably not identified because of the presence of boric acid, which might lower the pH at this low buffer capacity, inhibiting the oxidation of cocaine. In sample 9, 42% of levamisole was present, which suppresses the cocaine peak as well.<sup>12</sup> The analysis of these samples was repeated with microfluidic systems with a four times higher buffer capacity. The dotted lines in **Figure 6b** show the results and the successful appearance of the cocaine peak. For heroin (**Figure 6c**) all five samples showed a peak in the characteristic potential window at pH 5. **Figure 6d** depicts the superfingerprint of methamphetamine samples. All five samples showed no peak at pH 5 and a clear peak around 0.75 V at pH 12, similar to the measurements, of the standards. As shown by the results, the substances MDMA and heroin can be reliably detected at pH 5, while for cocaine and methamphetamine a buffer at pH 12 is required to identify the compound. The creation of the superfingerprint ensures that the characteristic peaks for each compound can be recorded without manual selection of the buffer. The new method also maintains a very

short operation time. The sample is dissolved in one ampoule and two measurements are performed in parallel.

In this work, we presented a successful design of a microfluidic dual pH sensor system. Future steps would include a stability study to research shelf life, to perform usability tests with end-users, and to fully integrate the electrodes in the microfluidic system by screen-printing directly on the films to reduce the cost price for large batches. Currently, the identification of the samples was based on the characteristic peak location of the drug compounds. However, the presence of the characteristic peak potentials of different cutting agents can also be used to substantiate the identification of the drug. For example, for confiscated samples of heroin there are many other electroactive substances present, while MDMA shows a very clean curve. Moreover, the multi-buffer voltammetric analysis system offers prospects for applying array-based pattern recognition algorithms such as principle component analysis, linear discriminant analysis and machine learning for improved recognition of the analytes.<sup>42,43</sup> The current application focused on the detection of illicit drugs in seized samples. Future work includes illicit drug detection in biofluids to be able to detect illicit drug use on-site as well. This requires lower detection limits which may be reached by electrode modifications. Lastly, the dual pH strategy can be applied in other voltammetry applications, such

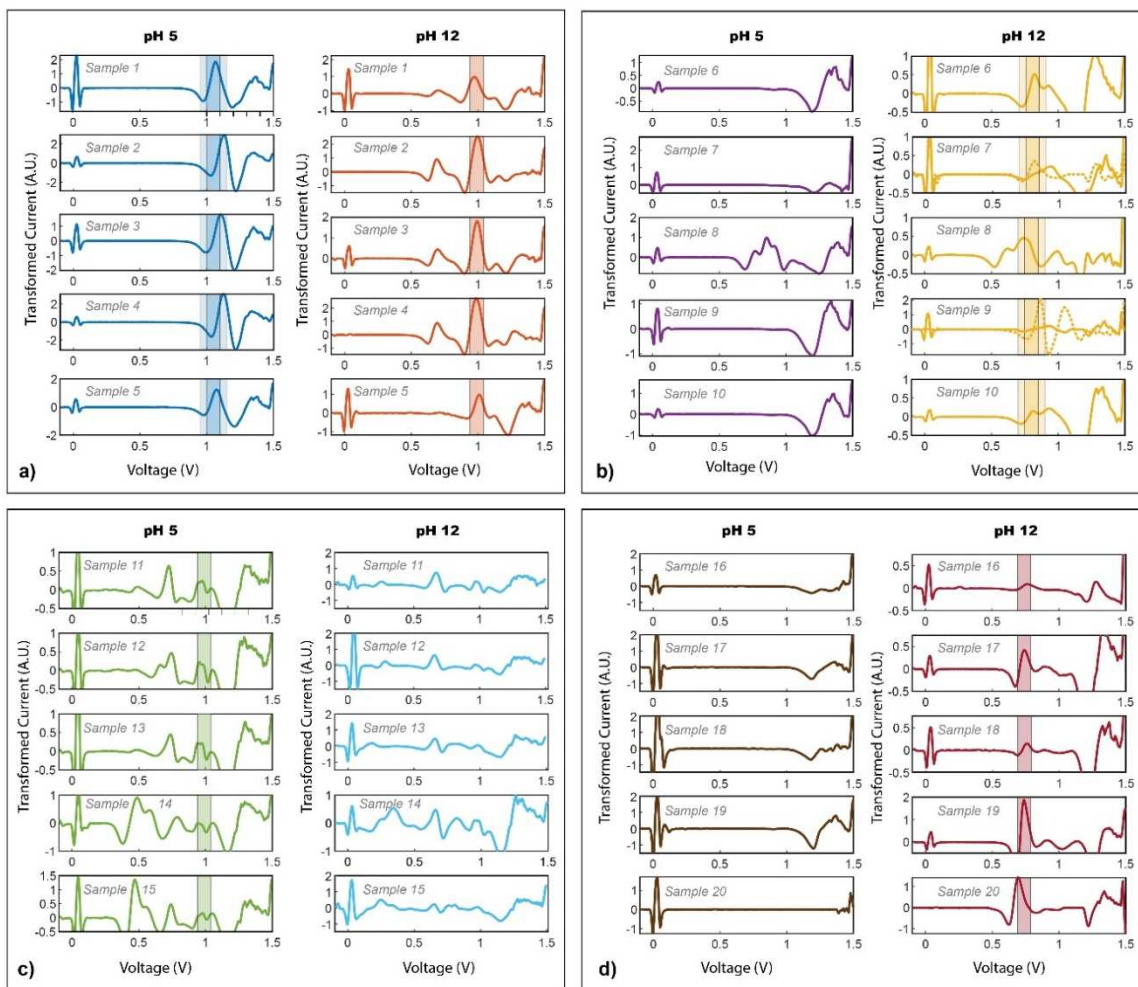


**Figure 6.** Electrochemical fingerprints of confiscated samples after applying the top-hat filter to the raw data. Superfingerprint of a) confiscated MDMA samples at pH 5 and 12, b) cocaine street samples c) heroin street samples and d) methamphetamine street samples. The colored bars show the potential windows based on the average results of the 1 mM standard solutions in the microfluidic systems. The dotted voltammograms for the cocaine samples are the results after increasing the buffer capacity four times.

as in the medical domain and food and nutrition domain, to derive more unique fingerprints of the analytes for reliable identification.

## Conclusion

This work presents the design of a microfluidic system for multi-channel voltammetric analysis of illicit drugs at different pHs. The sample is automatically brought to the desired pH in the buffer reservoirs, whereafter electrochemical measurements are performed in the sensor chamber. Real-time pH measurements in the sensor chamber showed that the sample reaches the desired pH value in 50 seconds. A proof-of-concept study was performed to detect four of the most common illicit drugs with square-wave voltammetry. By enabling electrochemical analysis at two pHs (5 and 12), characteristic superfingerprints of each drug were obtained. Measurements with drug standards in the microfluidic system showed that the characteristic peak potentials were reproducible. Furthermore, the feasibility of the concept was successfully explored with confiscated samples. To improve the drug detection of the more challenging samples, the buffer capacity should be optimized in future work to avoid pH variation at the surface of the electrode. The microfluidic electrochemical system thus simplifies the detection of illicit drugs in street samples by providing a single sampling procedure while maximizing the electrochemical information for a proper decision making process. Overall, the microfluidic device presents a leap forward on the voltammetric analysis of illicit drugs for rapid identification in decentralized settings by a non-expert user.

## ASSOCIATED CONTENT

### Supporting Information

The Supporting Information is available free of charge on the ACS Publications website.

Microfluidic system fabrication details, additional experimental results (PDF)

## AUTHOR INFORMATION

### Corresponding Author

\* corresponding author email address:  
karolien.dewael@uantwerpen.be

### Author Contributions

The manuscript was written through contributions of all authors. / All authors have given approval to the final version of the manuscript.

## ACKNOWLEDGMENT

This project received funding from the European Union's Horizon 2020 Research and Innovation Program BorderSens under the grant agreement No 833787. A.S. acknowledges funding through a Rubicon fellowship from the Dutch Research Council (File No. 019.223EN.003). M.P. acknowledges financial support from the Fund for Scientific Research (FWO) Flanders grant 1265223N.

## REFERENCES

1. *Drugs (psychoactive)*; World Health Organization: 2022.
2. *World Drug Report 2022*; United Nations Office on Drugs and Crime: 2022.
3. *European Drug Report 2022: Trends and Developments*; European Monitoring Centre for Drugs and Drug Addiction: Luxembourg, 2022.
4. Tsumura, Y.; Mitome, T.; Kimoto, S., False positives and false negatives with a cocaine-specific field test and modification of test protocol to reduce false decision. *Forensic Sci Int* **2005**, *155* (2-3), 158-164.

5. de Oliveira Penido, C. A. F.; Pacheco, M. T. T.; Lednev, I. K.; Silveira Jr, L., Raman spectroscopy in forensic analysis: identification of cocaine and other illegal drugs of abuse. *J Raman Spectrosc* **2016**, *47* (1), 28-38.
6. Dragan, A.-M.; Parrilla, M.; Feier, B.; Oprean, R.; Cristea, C.; De Wael, K., Analytical techniques for the detection of amphetamine-type substances in different matrices: A comprehensive review. *TrAC* **2021**, *145*, 116447.
7. Kranenburg, R. F.; Ou, F.; Sevo, P.; Petruzzella, M.; de Ridder, R.; van Klinken, A.; Hakkel, K. D.; van Elst, D. M. J.; van Veldhoven, R.; Pagliano, F.; van Asten, A. C.; Fiore, A., On-site illicit-drug detection with an integrated near-infrared spectral sensor: A proof of concept. *Talanta* **2022**, *245*, 123441.
8. Kranenburg, R. F.; Ramaker, H.-J.; van Asten, A. C., On-site forensic analysis of colored seized materials: Detection of brown heroin and MDMA-tablets by a portable NIR spectrometer. *Drug Test Anal* **2022**, *14* (10), 1762-1772.
9. de Jong, M.; Van Echelpoel, R.; Langley, A. R.; Eliaerts, J.; van den Berg, J.; De Wilde, M.; Somers, N.; Samyn, N.; De Wael, K., Real-time electrochemical screening of cocaine in lab and field settings with automatic result generation. *Drug Test Anal* **2022**, *14* (8), 1471-1481.
10. Florea, A.; Schram, J.; de Jong, M.; Eliaerts, J.; Van Durme, F.; Kaur, B.; Samyn, N.; De Wael, K., Electrochemical Strategies for Adulterated Heroin Samples. *Anal Chem* **2019**, *91* (12), 7920-7928.
11. Van Echelpoel, R.; Parrilla, M.; Slegers, N.; Shanmugam, S. T.; van Nuijs, A. L. N.; Slosse, A.; Van Durme, F.; De Wael, K., Validated portable device for the qualitative and quantitative electrochemical detection of MDMA ready for on-site use. *Microchem J* **2023**, *190*, 108693.
12. de Jong, M.; Florea, A.; Vries, A.-M. d.; van Nuijs, A. L. N.; Covaci, A.; Van Durme, F.; Martins, J. C.; Samyn, N.; De Wael, K., Levamisole: a Common Adulterant in Cocaine Street Samples Hindering Electrochemical Detection of Cocaine. *Anal Chem* **2018**, *90* (8), 5290-5297.
13. Dragan, A.-M.; Parrilla, M.; Slegers, N.; Slosse, A.; Van Durme, F.; van Nuijs, A.; Oprean, R.; Cristea, C.; De Wael, K., Investigating the electrochemical profile of methamphetamine to enable fast on-site detection in forensic analysis. *Talanta* **2023**, *255*, 124208.
14. Parrilla, M.; Slosse, A.; Van Echelpoel, R.; Felipe Montiel, N.; Langley, A. R.; Van Durme, F.; De Wael, K., Rapid On-Site Detection of Illicit Drugs in Smuggled Samples with a Portable Electrochemical Device *Chemosensors* **2022**.
15. Van Echelpoel, R.; de Jong, M.; Daems, D.; Van Espen, P.; De Wael, K., Unlocking the full potential of voltammetric data analysis: A novel peak recognition approach for (bio)analytical applications. *Talanta* **2021**, *233*.
16. Nielsen, J. B.; Hanson, R. L.; Almughamsi, H. M.; Pang, C.; Fish, T. R.; Woolley, A. T., Microfluidics: Innovations in Materials and Their Fabrication and Functionalization. *Anal Chem* **2020**, *92* (1), 150-168.
17. Raj M, K.; Chakraborty, S., PDMS microfluidics: A mini review. *J Appl Polym Sci* **2020**, *137* (27), 48958.
18. Focke, M.; Kosse, D.; Müller, C.; Reinecke, H.; Zengerle, R.; von Stetten, F., Lab-on-a-Foil: microfluidics on thin and flexible films. *Lab Chip* **2010**, *10* (11), 1365-1386.
19. Noviana, E.; Ozer, T.; Carrell, C. S.; Link, J. S.; McMahon, C.; Jang, I.; Henry, C. S., Microfluidic Paper-Based Analytical Devices: From Design to Applications. *Chem Rev* **2021**, *121* (19), 11835-11885.
20. Kim, T. H.; Hahn, Y. K.; Kim, M. S. Recent Advances of Fluid Manipulation Technologies in Microfluidic Paper-Based Analytical Devices ( $\mu$ PADs) toward Multi-Step Assays *Micromachines* [Online], 2020.
21. Lee, C.-Y.; Wang, W.-T.; Liu, C.-C.; Fu, L.-M., Passive mixers in microfluidic systems: A review. *Chem Eng J* **2016**, *288*, 146-160.
22. Khosravi Parsa, M.; Hormozi, F.; Jafari, D., Mixing enhancement in a passive micromixer with convergent-divergent sinusoidal microchannels and different ratio of amplitude to wave length. *Comput Fluids* **2014**, *105*, 82-90.
23. Liosis, C.; Sofiadis, G.; Karvelas, E.; Karakasidis, T.; Sarris, I. A Tesla Valve as a Micromixer for Fe<sub>3</sub>O<sub>4</sub> Nanoparticles *Processes* **2022**.
24. Fang, Y.; Ye, Y.; Shen, R.; Zhu, P.; Guo, R.; Hu, Y.; Wu, L., Mixing enhancement by simple periodic geometric features in microchannels. *Chem Eng J* **2012**, *187*, 306-310.
25. Nimafar, M.; Viktorov, V.; Martinelli, M., Experimental comparative mixing performance of passive micromixers with H-shaped sub-channels. *Chem Eng Sci* **2012**, *76*, 37-44.
26. Nguyen, V.-T.; Song, S.; Park, S.; Joo, C., Recent advances in high-sensitivity detection methods for paper-based lateral-flow assay. *Biosens Bioelectron* **2020**, *152*, 112015.
27. Bahadır, E. B.; Sezgintürk, M. K., Lateral flow assays: Principles, designs and labels. *TrAC* **2016**, *82*, 286-306.

28. Sena-Torralba, A.; Álvarez-Diduk, R.; Parolo, C.; Piper, A.; Merkoçi, A., Toward Next Generation Lateral Flow Assays: Integration of Nanomaterials. *Chem Rev* **2022**, *122* (18), 14881-14910.
29. Fu, E.; Liang, T.; Spicar-Mihalic, P.; Houghtaling, J.; Ramachandran, S.; Yager, P., Two-Dimensional Paper Network Format That Enables Simple Multistep Assays for Use in Low-Resource Settings in the Context of Malaria Antigen Detection. *Anal Chem* **2012**, *84* (10), 4574-4579.
30. Zimmermann, M.; Schmid, H.; Hunziker, P.; Delamarche, E., Capillary pumps for autonomous capillary systems. *Lab Chip* **2007**, *7* (1), 119-125.
31. Comsol Capillary Filling — Level Set Method. [https://doc.comsol.com/5.6/doc/com.comsol.help.models.mfl.capillary\\_filling\\_ls/models.mfl.capillary\\_filling\\_ls.pdf](https://doc.comsol.com/5.6/doc/com.comsol.help.models.mfl.capillary_filling_ls/models.mfl.capillary_filling_ls.pdf) (accessed 19 July 2023).
32. Mazzara, F.; Patella, B.; D'Agostino, C.; Bruno, M. G.; Carbone, S.; Lopresti, F.; Aiello, G.; Torino, C.; Vilasi, A.; O'Riordan, A.; Inguanta, R. PANI-Based Wearable Electrochemical Sensor for pH Sweat Monitoring *Chemosensors* [Online], 2021.
33. Parrilla, M.; Vanhooydonck, A.; Johns, M.; Watts, R.; De Wael, K., 3D-printed microneedle-based potentiometric sensor for pH monitoring in skin interstitial fluid. *Sens Actuators B Chem* **2023**, *378*, 133159.
34. Zumdahl, S., Applications of Aqueous Equilibria. In *Chemical Principles*, D.C. Heath and Company: Canada, 1995; pp 302-303.
35. A.S.M. Steijlen, M. P., R. Van Echelpoel, K. De Wael, A Microfluidic Platform for Selective On-site Electrochemical Identification of Illicit Drugs. In *Miniaturized Systems for Chemistry and Life Sciences (μTAS 2023)*, Katowice, 2023.
36. Vittal, R.; Gomathi, H.; Kim, K.-J., Beneficial role of surfactants in electrochemistry and in the modification of electrodes. *Adv Colloid Interface Sci* **2006**, *119* (1), 55-68.
37. Parrilla, M.; Joosten, F.; De Wael, K., Enhanced electrochemical detection of illicit drugs in oral fluid by the use of surfactant-mediated solution. *Sens Actuators B Chem* **2021**, *348*, 130659.
38. de Jong, M.; Slegers, N.; Schram, J.; Daems, D.; Florea, A.; De Wael, K., A Benzocaine-Induced Local Near-Surface pH Effect: Influence on the Accuracy of Voltammetric Cocaine Detection. *Analysis & Sensing* **2021**, *1* (1), 54-62.
39. Felipe Montiel, N.; Parrilla, M.; Beltrán, V.; Nuyts, G.; Van Durme, F.; De Wael, K., The opportunity of 6-monoacetylmorphine to selectively detect heroin at preanodized screen printed electrodes. *Talanta* **2021**, *226*, 122005.
40. Fiorentin, T. R.; Krotulski, A. J.; Martin, D. M.; Browne, T.; Triplett, J.; Conti, T.; Logan, B. K., Detection of Cutting Agents in Drug-Positive Seized Exhibits within the United States. *J Forensic Sci* **2019**, *64* (3), 888-896.
41. Van Echelpoel, R.; de Jong, M.; Daems, D.; Van Espen, P.; De Wael, K., Unlocking the full potential of voltammetric data analysis: A novel peak recognition approach for (bio)analytical applications. *Talanta* **2021**, *233*, 122605.
42. Dean, S. N.; Shriver-Lake, L. C.; Stenger, D. A.; Erickson, J. S.; Golden, J. P.; Trammell, S. A. Machine Learning Techniques for Chemical Identification Using Cyclic Square Wave Voltammetry *Sensors* **2019**.
43. Cetó, X.; Céspedes, F.; del Valle, M., Comparison of methods for the processing of voltammetric electronic tongues data. *Microchim Acta* **2013**, *180* (5), 319-330.